PHYSICAL REVIEW B **72**, 220403(R) (2005)

Anticorrelation between ferromagnetism and ferroelectricity in perovskite manganites

T. Goto,[1] Y. Yamasaki,[1] H. Watanabe,[1] T. Kimura,[2] and Y. Tokura[1,3,4]
[1]*Department of Applied Physics, University of Tokyo, Tokyo 113-8656, Japan*
[2]*Bell Laboratories, Lucent Technologies, 600 Mountain Avenue, Murray Hill, New Jersey 07974, USA*
[3]*Spin Superstructure Project (SSS), ERATO, Japan Science and Technology Agency (JST), Tsukuba 305-8562, Japan*
[4]*Correlated Electron Research Center (CERC), National Institute of Advanced Industrial Science and Technology (AIST), Tsukuba 305-8562, Japan*
(Received 17 October 2005; published 9 December 2005)

Magnetic and dielectric properties have been investigated for a mixed-crystal system $Tb_{1-x}Gd_xMnO_3$ in between $TbMnO_3$ with ferroelectric and incommensurate antiferromagnetic (AFM) orders and $GdMnO_3$ with paraelectric and canted AFM (weakly ferromagnetic) states, as functions of x, temperature T, and magnetic field B applied along the c axis. A systematic study on the magnetic and electric phase diagrams in the x-T, B-T, and x-B planes has revealed important interplay between Mn d-electron spins and Gd f-electron moments. A clear anticorrelation between the (weak) ferromagnetism and the ferroelectricity is observed near the phase boundaries.

DOI: 10.1103/PhysRevB.72.220403 PACS number(s): 75.47.Lx, 75.80.+q, 75.25.+z, 75.30.Kz

The gigantic magnetoelectric (ME) effect,[1,2] which is the efficient induction of the polarization P (magnetization M) by external magnetic field B (electric field E), has recently been of vital interest from viewpoints of electronic origin of ferroelectrics as well as possible spin-electron application. The consensus for the strategy to realize the gigantic ME effect is the use of multiferroics, i.e., materials in which ferroelectricity and antiferromagnetism can coexist. The $B(E)$-field-induced phase change to the spontaneous M (P) phase may simultaneously accompany the switching of the other property P (M). Concerning such phase control in multiferroics, a recent observation of gigantic ME effect in perovskite $TbMnO_3$ provides an intriguing approach to the magnetic control of electric polarization.[3] In $TbMnO_3$, the ferroelectricity appears to originate from long-period (incommensurate) antiferromagnetic (AFM) orders (spiral or ellipsoidal)[4] that cause twice-period lattice modulations through magnetoelastic coupling. The ionic radius of Tb^{3+} in $TbMnO_3$ is appropriate to realize the incommensurate AFM (ICAFM) structures[5,6] by tuning the spin frustration arising from the competing nearest-neighbor and next-nearest-neighbor exchange interactions between Mn^{3+} d-electron spins in the ab plane of the orthorhombic lattice.[7] On the other hand, in $GdMnO_3$, whose Gd atom locates adjacent to Tb in the Periodic Table; the canted AFM state (A-type-AFM with the ab-plane ferromagnetic spin order) with a weak ferromagnetic (WFM) moment ($\sim 0.2\mu_B$/Mn) along the c axis is the ground state,[7] while the compound remains paraelectric (PE) in the whole temperature (T) range.[8–11]

In this paper, we demonstrate the magnetoelectric phase control based on the anticorrelation between the (weak) ferromagnetism and the ferroelectricity in a mixed-crystal system $Tb_{1-x}Gd_xMnO_3$, which is summarized in Fig. 1. We show how rare-earth f-electron moments affect magnetic and electric properties in the multiferroic rare-earth manganites. Tb^{3+} ($4f^8$) is of Ising-like anisotropy, while Gd^{3+} ($4f^7$) without orbital angular momentum is of a Heisenberg one. In $TbMnO_3$, the Tb^{3+} moments are along either of two Ising axes within the ab plane at 57° off the b axis.[5] Thus, the gigantic ME effects upon applying magnetic fields along the a and b axes (the magnetic-field-induced electric polarization flop) are likely to be triggered by the magnetic reversal of Ising Tb^{3+} moments.[9] By contrast, the application of magnetic fields along the c axis (up to $\sim$14 T) hardly directs the Tb^{3+} moments along the c axis, therefore the observed magnetic-field-induced suppression of ferroelectricity with the $B \| c$ configuration is likely to be related to a metamagnetic transition of Mn spins alone.[9] In the present study we show that partially substituted Gd^{3+} moments strongly affect the $B(\| c)$ induced suppression of ferroelectricity via exchange interaction between Gd(f) and Mn(d) moments, and present the anomalous magnetoelectric phase diagram for $Tb_{1-x}Gd_xMnO_3$.

A series of $Tb_{1-x}Gd_xMnO_3$ ($0 \leqslant x \leqslant 1$) single crystals were grown by the floating zone method. Powder x-ray diffraction measurements confirmed that all the crystals investigated here show the *Pbnm* orthorhombic structure at room temperature. The crystals were oriented by Laue x-ray diffraction patterns and cut into thin plates. Silver was vacuum deposited onto the widest faces of the plates to form the capacitor electrodes. The dielectric constant ϵ was measured by using an LCR meter (Hewlett-Packard, 4274A). The electric polarization P was obtained by integration of the pyroelectric (or magnetoelectric) current which was measured with an electrometer. Magnetization M was measured with a dc magnetometer. Magnetic field B up to 14 T was applied along the c axis in this study.

In Fig. 2, we show the temperature (T) dependence of ϵ and P along the c and a axes for $Tb_{1-x}Gd_xMnO_3$. As shown in Figs. 2(b) and 2(d), the finite spontaneous polarization appears along the c axis in the $x \leqslant 0.6$ crystals, while the crystals with $0.6 \leqslant x \leqslant 0.8$ were found to possess a ferroelectric phase with P along the a axis in an intermediate T region. It is obvious from the comparison with these polarization data that sharp peak structures in the ϵ-T curves [indicated by open triangles in Figs. 2(a) and 2(c)] correspond to the ferroelectric (FE) transitions. The sharp peak is

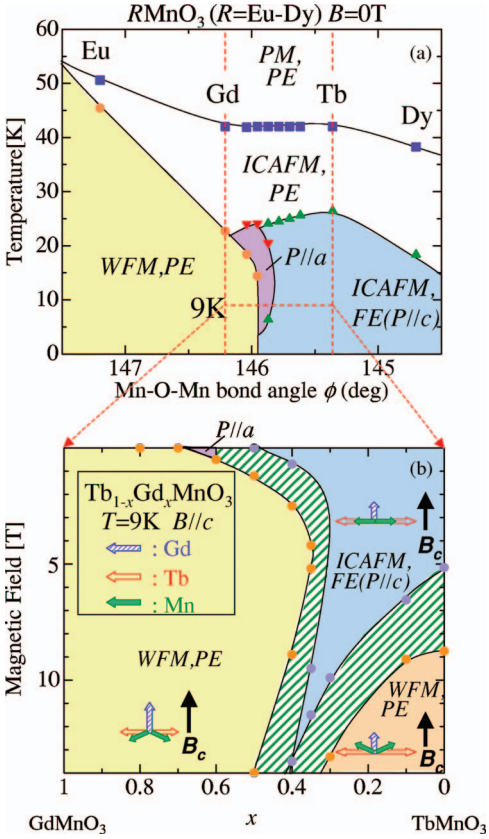

FIG. 1. (Color) (a) Phase diagram of the perovskite rare-earth manganites as a function of Mn-O-Mn bond angle. The incommensurate antiferromagnetic (ICAFM) phase undergoes the transition to the ferroelectric (FE) state with lowering temperature, while the *A*-type AFM phase (WFM) with the weak ferromagnetic moment ($\sim 0.2\mu_B$/Mn) along the *c* axis remains paraelectric (PE). (b) Magnetoelectric phase diagram in the *x*-$B(\|c)$ plane for $Tb_{1-x}Gd_xMnO_3$ at 9 K. Hatched areas denote the hysteresis regions. The insets show schematic magnetic configurations on Gd, Tb, and Mn moments relative to $B(\|c)$ at the respective phases (see text and Ref. 12). The phase boundaries were determined from anomalies in magnetization, dielectric constant, and/or electric polarization.

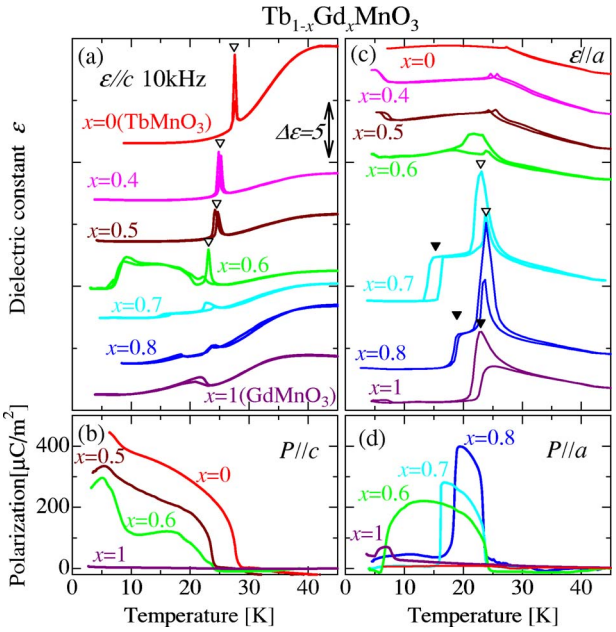

FIG. 2. (Color online) Temperature dependence of dielectric constant ϵ and polarization *P* parallel to the *a* axis or *c* axis in $Tb_{1-x}Gd_xMnO_3$ at zero magnetic field. Open and closed triangles in (a) and (c) denote the transitions into ferroelectric and *A*-type AFM phases, respectively.

seen in $\epsilon(\|c)$ of low *x* (<0.6) or in $\epsilon(\|a)$ of intermediate *x* ($0.6<x<0.8$). Incidentally, we also observed another remarkable anomaly, i.e., a stepwise change, in $\epsilon(\|a)$-*T* curves of $x=0.7$ and 0.8 crystals [indicated by closed triangles in Fig. 2(c)]. This anomaly corresponds to a reentrant transition to a low-*T* PE phase [compare Fig. 2(c) with Fig. 2(d)]. To sum up, the evolution of ferroelectric properties at $B=0$ is displayed in Fig. 1(a) as the phase diagram in the Mn-O-Mn bond angle (ϕ) vs *T* plane.[12] In between the paraelectric $GdMnO_3$ and the ferroelectric $TbMnO_3$ with *P* along the *c* axis, there exists a distinct ferroelectric phase with *P* along the *a* axis.[13]

We exemplify in Fig. 3 the magnetic field effect on the dielectric properties for the $x=0.5$ crystal, in which the close correlation can be seen between magnetism and ferroelectricity. Figures 3(a)–3(c) display the *T* dependence of $M(\|c)$, $\epsilon(\|a)$, and $P(\|c)$ at selected values of *B* applied along the *c* axis. As shown in Fig. 3(c), the $x=0.5$ crystal does show ferroelectricty below ~ 25 K. However, the application of $B(\|c)$ gives rise to a reentrant transition into a low-*T* PE state. The triangles in the figure indicate the temperature (T_{PE}) of the transition from the FE to the low-*T* PE phase. It should be noted that the T_{PE} does not change monotonically with increasing *B*: T_{PE} (~ 13 K at 1 T) increases with increasing *B*, reaches a maximum (~ 18 K) at ~ 6 T, and then above ~ 6 T tends to decrease. In Figs. 3(d)–3(f), we show the isothermal *B* dependence of $M(\|c)$, $\epsilon(\|a)$, and $P(\|c)$ at $T=4.2$ K and 15 K. [For the measurement of the *P*-*H* curves, an electric field (~ 200 kV/m) was applied during the measurement to keep the crystal in the single domain state of the ferroelectric phase.] Corresponding to the anomalies in *M*-*H* curves, ϵ and *P* show abrupt changes. Thus, the suppression of the ferroelectric order induced by *B* appears to be closely tied with a change of the magnetic structure. Namely, the ferroelectric order disappears when the weak ferromagnetic moment appears along the *c* axis, and vice versa. Here, it is to be emphasized that the WFM-PE state induced by *B* is accompanied by fully ferromagnetic Mn spin alignment in the *ab* plane that cannot host the incommensurate spin-order induced FE state.

To investigate the systematic variation of the stability of the ferroelectric phase, we display in Fig. 4 the magnetoelectric phase diagrams in the *B*-*T* plane with varying *x*. The phase boundaries in the diagrams were obtained from the *T* and *B* profiles of *M*, ϵ, and *P*.[15] Note that the first-order transition between incommensurate antiferromagnetic and ferroelectric (ICAFM-FE) and weak ferromagnetic and paramagnetic (WFM-PE) phases is accompanied by a hysteresis region (hatched areas in Fig. 4). The phase diagrams confirm that the appearance of WFM order along the *c* axis suppresses the FE order in this system. The disappearance of

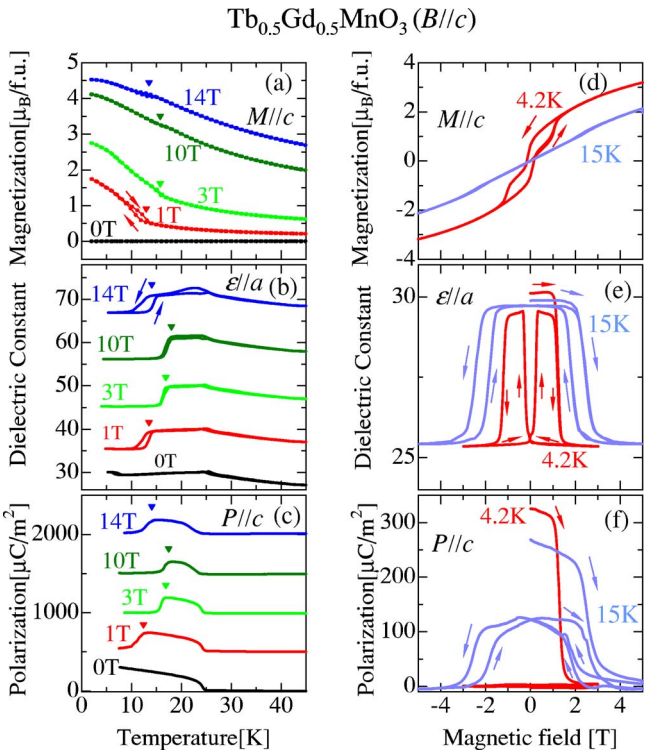

FIG. 3. (Color online) Magnetic field ($B\|c$) effect on the magnetization $M(\|c)$, the dielectric constant $\epsilon(\|a)$, and the polarization $P(\|c)$ for $Tb_{0.5}Gd_{0.5}MnO_3$. (a)–(c) The temperature dependence at several fixed magnetic fields. The respective curves in (b) and (c) are displaced vertically for clarity, by (b) $\Delta\epsilon=10$ and (c) $\Delta P=500\ \mu C/m^2$, with increasing B values. The triangles indicate the anomalies (at T_{PE}) accompanied by the reentrant transition to low-T paraelectric phase. (d)–(f) Magnetic field dependence at $T=4.2$ K and 15 K.

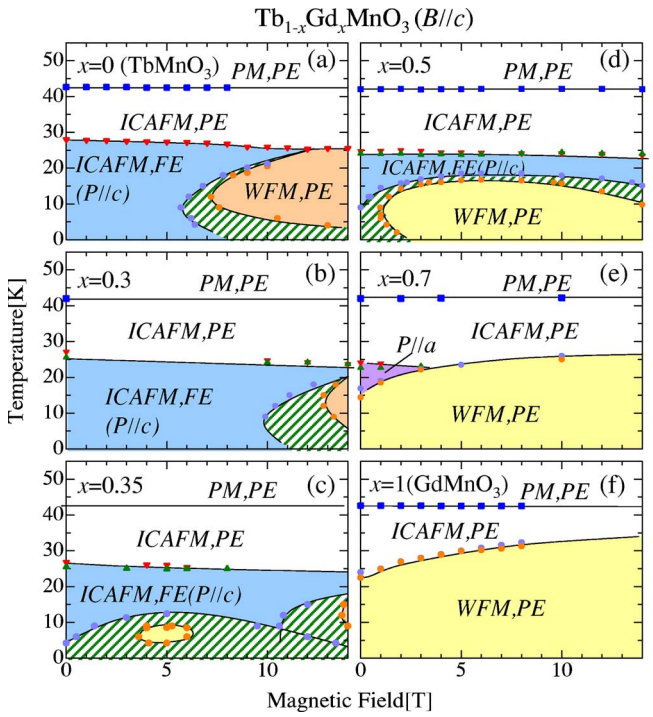

FIG. 4. (Color online) Magnetoelectric phase diagrams of $Tb_{1-x}Gd_xMnO_3$ ($x=0$, 0.3, 0.35, 0.5, 0.7, and 1). PM, ICAFM, WFM, PE, and FE stand for paramagnetic, incommensurate antiferromagnetic, weak ferromagnetic, paraelectric, and ferroelectric states, respectively. Hatched areas denote the hysteresis regions.

ferroelectricity in a high magnetic field along the c axis in $TbMnO_3$ (Ref. 9) has been discussed in terms of the transition to WFM with a weak ferromagnetic moment along the c axis due to the Dzyaloshinskii-Moriya interaction.[16,17] Then, it might be anticipated that the high-B WFM-PE phase in the $TbMnO_3(x=0)$ crystal would monotonously expand toward a lower-B region with increasing x, because the A-type AFM phase (WFM) should be stabilized toward the $B=0$ ground state in $GdMnO_3(x=1)$. As shown in Figs. 4(a)–4(c), however, the high-B WFM-PE phase is rather shifted toward a higher B region with increasing x. Then, another WFM-PE phase shows up at around 7 K and 5 T in the $x=0.35$ crystal, as seen in Fig. 4(c). With further increasing x, this low-B WFM-PE phase grows and is smoothly connected with the WFM-PE (the canted A-type AFM) phase in $GdMnO_3$.

We summarize the magnetic field effect ($B\|c$) on the dielectric properties in $Tb_{1-x}Gd_xMnO_3$ by showing the ME phase diagram at 9 K in the x-B plane in Fig. 1(b). It is obvious that the low-B WFM-PE phase in $GdMnO_3$ side (yellow colored area) and the high-B WFM-PE phase in $TbMnO_3$ side (orange colored area) are not smoothly connected, but intervened by the ICAFM-FE phase (blue area). In $TbMnO_3(x=0)$, the application of $B(\|c)\sim 8$ T causes a phase transition to the high-B WFM-PE phase. The onset field for the phase transition steeply increases with increasing x [see the orange area in Fig. 1(b)]. Thus, it seems that there exist two distinct WFM-PE phases in the $Tb_{1-x}Gd_xMnO_3$ system.

To understand the complex ME phase diagrams in $Tb_{1-x}Gd_xMnO_3$, in particular the existence of the two distinct WFM-PE phases [yellow and orange colored areas in Fig. 1(b)], we should take account of the difference between the magnetic properties of Tb^{3+} and Gd^{3+} ions. The Ising-like Tb^{3+} f-electron moments in $TbMnO_3$ have two easy axes within the ab plane.[5] Therefore, the Tb^{3+} f-electron moments contribute little to $M(\|c)$ of $TbMnO_3$ and hence to the transition to the WFM-PE phase when B is applied along c. By contrast, in the Gd^{3+} moments ($4f^7$) without orbital angular momentum, the Gd^{3+} moments (Heisenberg-like) can, unlike the Tb^{3+} ones, contribute to $M(\|c)$) and work as an internal magnetic field on Mn spins in $Tb_{1-x}Gd_xMnO_3$. According to a recent report by Hemberger *et al.*,[18] the Gd^{3+} moments in $GdMnO_3$ are polarized antiferromagnetically with respect to the weak ferromagnetic component (along the c axis) of the Mn moments. The moment configuration of the low-B WFM-FE phase in a higher x (Gd-rich) region is illustrated in the inset on the yellow-colored region of Fig. 1(b). In a higher x region, the application of $B(\|c)$) directs the Gd^{3+} moments along the c axis at first, while the Mn^{3+} moments along the opposite direction due to the antiferromagnetic f-d interaction. Meanwhile, in the high-B WFM-PE phase in a lower x (Tb-rich) region, the canted weak ferromagnetic moment on Mn^{3+} ions dominates $M(\|c)$ [see the inset on the orange-colored region in Fig. 1(b)]. Thus, the difference be-

tween the two distinct WFM-PE phases reflects the different direction of the weak ferromagnetic moments on Mn sites, i.e., parallel or antiparallel to external magnetic fields.

The above feature also explains why the onset field of the transition from the ICAFM-FE to the high-B WFM-PE phases increases with increasing x. The exchange interaction between the Gd^{3+} and Mn^{3+} moments is antiferromagnetic in nature. As shown in the inset on the orange-colored region in Fig. 1(b), however, the Gd^{3+} moments in the high-B WFM-PE phase are likely to align parallel to the weak ferromagnetic moment on Mn^{3+}. The increasing Gd substitution (up to $x=0.4$) on the Tb site in $TbMnO_3$ gives rise to an internal magnetic field in the opposite direction to external magnetic fields, and hence increases the critical magnetic field of the transition from the ICAFM-FE to the high-B WFM-PE phases, as observed.

In summary, the anticorrelation between the (weak) ferromagnetism and the ferroelectricity has been demonstrated for $Tb_{1-x}Gd_xMnO_3$ when magnetic fields are applied along a specific direction (the c axis in the *Pbnm* notation). We have revealed the existence of two weak ferromagnetic and paraelectric phases with different magnetic coupling between Gd^{3+} and Mn^{3+} moments. The difference in the magnetic configurations produces the complex phase transition phenomena not only in magnetic properties but also in electric ones such as a reentrant ferroelectric transition. The present results suggest that the ferroelectricity in rare-earth manganites can be controlled in a more versatile way by tuning the f-d interaction between rare-earth and Mn moments.

We thank T. Arima for helpful discussions. This work was in part supported by JSPS KAKENHI (Contract Nos. 17340104, 15104006) and MEXT TOKUTEI (Contract No. 16076205).

[1] M. Fiebig, J. Phys. D **38**, R123 (2005).

[2] H. Schmid, Ferroelectrics **62**, 317 (1994); **221**, 9 (1999).

[3] T. Kimura, T. Goto, H. Shintani, K. Ishizaka, T. Arima, and Y. Tokura, Nature (London) **426**, 55 (2003).

[4] M. Kenzelmann, A. B. Harris, S. Jonas, C. Broholm, J. Schefer, S. B. Kim, C. L. Zhang, S.-W. Cheong, O. P. Vajk, and J. W. Lynn, Phys. Rev. Lett. **95**, 087206 (2005).

[5] S. Quezel, F. Tcheou, J. Rossat-Mignod, G. Quezel, and E. Roudaut, Physica B **86–88**, 916 (1977).

[6] R. Kajimoto, H. Yoshizawa, H. Shintani, T. Kimura, and Y. Tokura, Phys. Rev. B **70**, 012401 (2004); **70**, 219904(E) (2004).

[7] T. Kimura, S. Ishihara, H. Shintani, T. Arima, K. T. Takahashi, K. Ishizaka, and Y. Tokura, Phys. Rev. B **68**, 060403(R) (2003).

[8] Concerning the ferroelectric feature, contradictory data have been reported in Refs. 9–11. One of them showed the spontaneous polarization along the a axis (P_a) at the zero-field ground state (Ref. 11), while the others reported the substantial P_a can only be observed when a magnetic field is applied along the b axis (Refs. 9 and 10). The discrepancy of the reported results may be explained in terms of the slight off-stoichiometry of the samples, since the Mn-O-Mn bond angle ϕ of $GdMnO_3$ resides on the immediate vicinity of the boundary between paraelectric canted A-type AFM and ferroelectric long-period AFM phases in the ϕ-T phase diagram [see Fig. 1(a)].

[9] T. Kimura, G. Lawes, T. Goto, Y. Tokura, and A. P. Ramirez, Phys. Rev. B **71**, 224425 (2005).

[10] A. M. Kadomtseva, Yu. F. Popov, G. P. Vorob'ev, K. I. Kamilov, A. P. Pyatakov, V. Yu. Ivanov, A. A. Mukhin, and A. M. Balbashov, JETP Lett. **81**, 22 (2005).

[11] K. Noda, S. Nakamura, J. Nagayama, and H. Kuwahara, J. Appl. Phys. **97**, 10C103 (2005).

[12] According to recent studies of neutron diffraction (Ref. 4), the paraelectric (PE) ICAFM shows the collinear ($\|b$) spin structure, which turns into the spiral (bc plane) structure in the ferroelectric (FE) state. In this paper, however, the magnetic structure in the incommensurate antiferromagnetic phase is schematically illustrated in the simplest manner as in Fig. 1(b) for simplicity.

[13] A similar a-polarized phase also shows up in $TbMnO_3$ when B is applied along the b axis. A recent x-ray study (Ref. 14) has revealed the commensurate magnetic q-vector $\left[0\ \frac{1}{4}\ 1\right]$ in the *Pbnm* setting for the $P\|a$ phase.

[14] T. Arima, T. Goto, Y. Yamasaki, S. Miyasaka, K. Ishii, M. Tsubota, T. Inami, Y. Murakami, and Y. Tokura, Phys. Rev. B **72**, 100102(R) (2005).

[15] The phase boundaries for PM,PE$\leftrightarrow$ICAFM,PE$\leftrightarrow$ICAFM,FE transitions were derived from the T-scan measurements at constant B, and those for ICAFM,FE$\leftrightarrow$WFE,PE ones were from the T- or B-scan measurements.

[16] I. Solovyev, N. Hamada, and K. Terakura, Phys. Rev. Lett. **76**, 4825 (1996).

[17] V. Skumryev, F. Ott, J. M. D. Coey, A. Anane, J.-P. Renard, L. Ponsard-Gaudart, and A. Revcolevschi, Eur. Phys. J. B **11**, 401 (1999).

[18] J. Hemberger, S. Lobina, H.-A. Krug von Nidda, N. Tristan, V. Yu. Ivanov, A. A. Mukhin, A. M. Balbashov, and A. Loidl, Phys. Rev. B **70**, 024414 (2004).